Supporting Information

Persistent luminescence of zinc gallogermanates

Celina Matuszewska, Tomasz W. Pańczuk, Peter A. Tanner,* Ka-Leung Wong*

* Corresponding authors

Department of Chemistry, Hong Kong Baptist University, Kowloon Tong, Hong Kong S.A.R.

Table of contents

Text S1. Equations for tunneling processes

In various reports, the dependence of various parameters upon isothermal luminescence have been studied, with intensity at time *t* following the relation:[1,2]

$$I(t) = \frac{A}{(1 + B \cdot t)^C} \tag{S1}$$

where *A* represents the initial intensity I_0; *B* and *C* are constants, all parameters depend upon the irradiation and experimental conditions. These dependences were given empirically, for low dose rate as:[1,2]

$$C = 1 + a/R \tag{S2}$$

where *a* is a constant and *R* is the dose rate (charging power);

$$I_0 = A = b \cdot R \cdot t^{1/4} \tag{S3}$$

where *b* is a constant and *t* is the irradiation time; and:

$$B = c \cdot R \cdot t^{1/2} \tag{S4}$$

where *c* is a constant.

Text S2. Kitis Equation for fitting a single glow curve with the general kinetics model.[3]

$$y = I \cdot b^{\frac{b}{b-1}} \cdot exp(\frac{E}{0.695x} \cdot \frac{x - T_M}{T_M}) \cdot \left((1 + (b-1) \cdot \left(2 \cdot 0.695 \cdot \frac{T_M}{E}\right) + (b-1) \cdot (1 - 2 \cdot 0.695 \cdot \frac{T_M}{E}) \right. \quad \text{(S5)}$$

Here, y represents the counts at temperature x (K); E is the activation energy in cm^{-1} since the value 0.695 cm^{-1} K^{-1} has been taken for the Boltzmann factor, k. I is the maximum intensity, b the kinetics order, T_M is the maximum temperature (K). Hence there are four parameters derived from the fit: E, b, T_M, I.

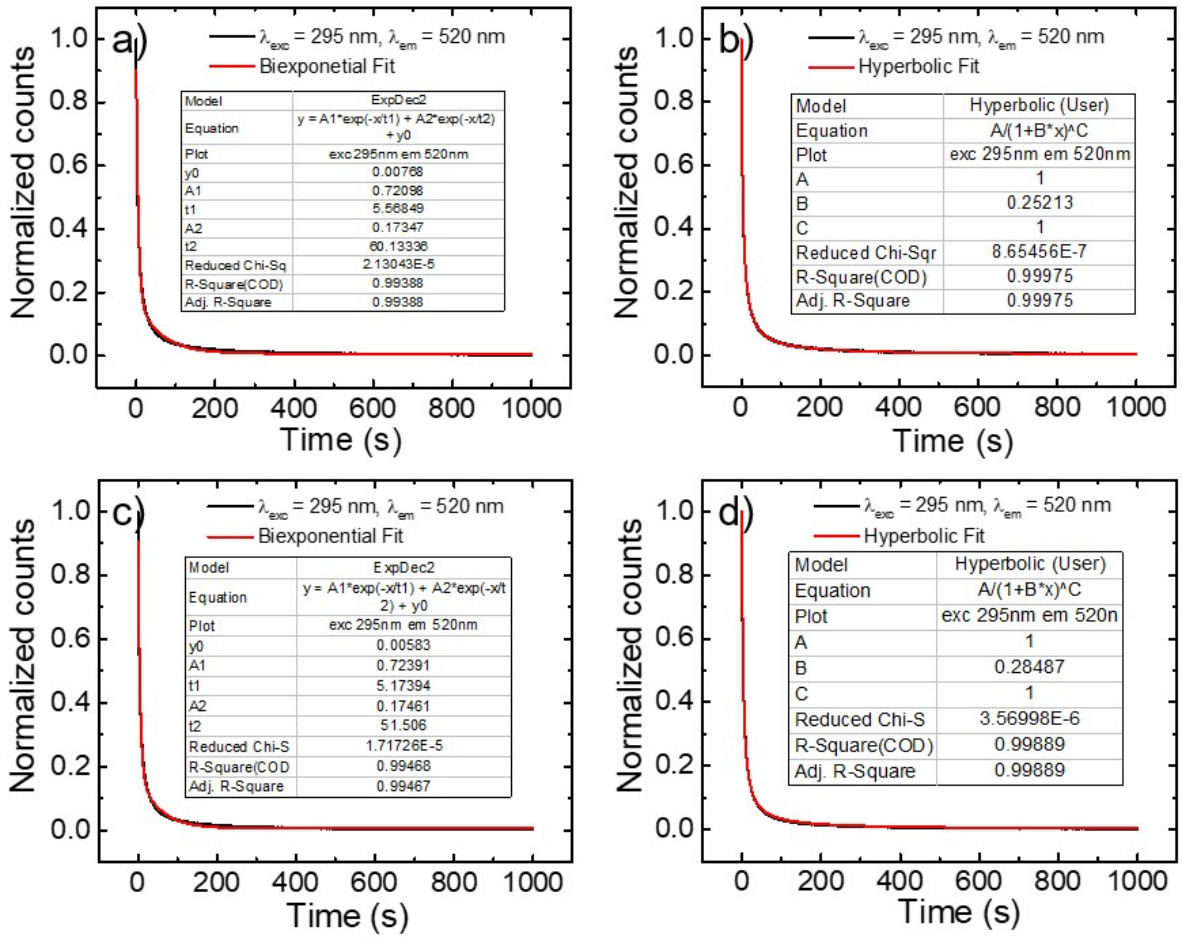

Figure S1. Selected room temperature persistent luminescence decays with biexponential and hyperbolic fits for zinc gallogermanate samples with different zinc contents presented in Figure 2b. Prior to the fitting, all decay curves were normalized to the value of unity, i.e., the parameter *A* in Eq. 3 was set as unity in each case.

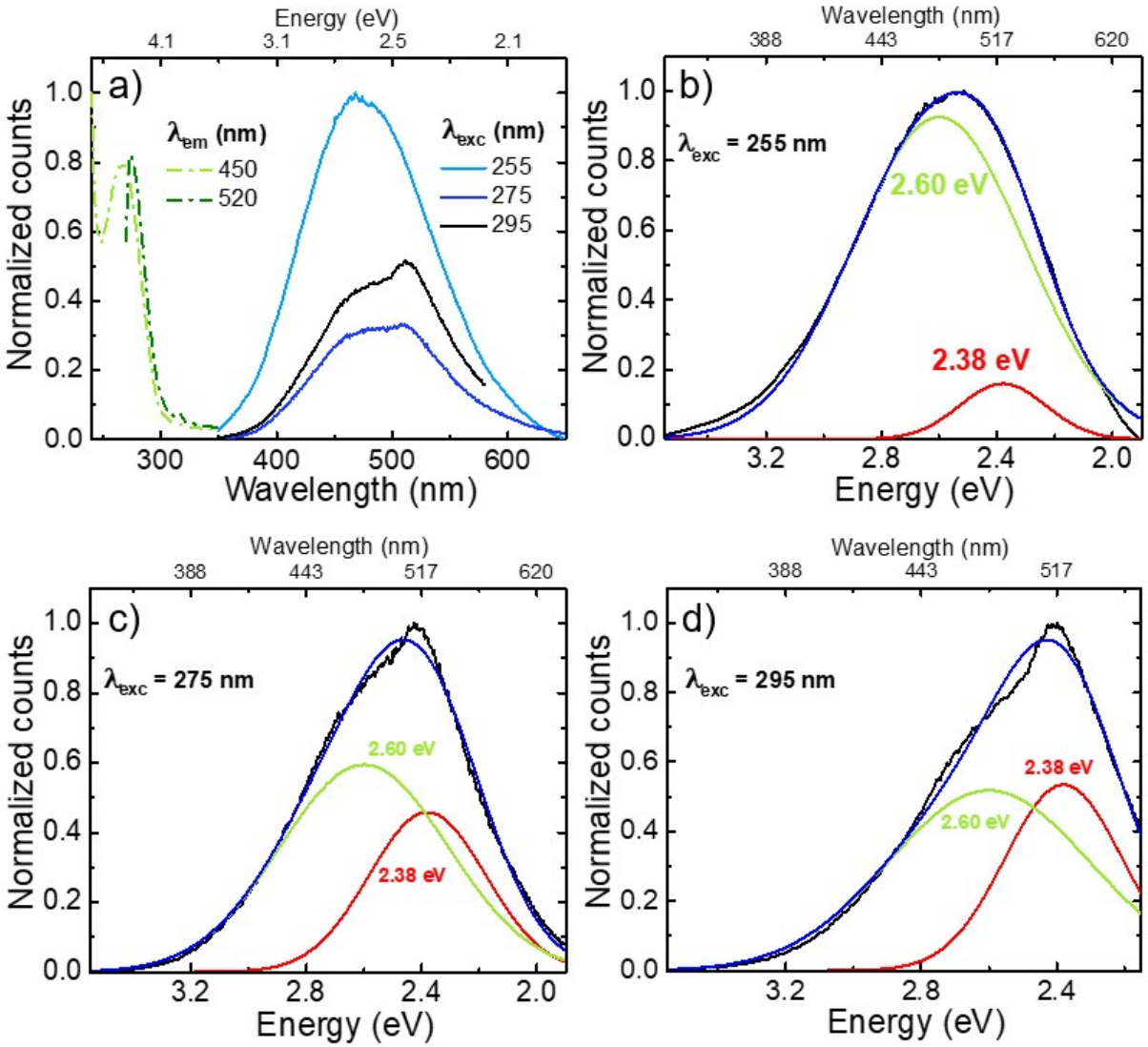

Figure S2. Photoluminescence spectra of $Zn_3Ga_2Ge_2O_{10}$ at room temperature: a) emission spectra for λ_{exc} = 255, 275, 295 nm and excitation spectra for λ_{em} = 450, 520 nm; b) deconvolution of emission spectra measured under 255 nm excitation; c) deconvolution of emission spectra measured under 275 nm excitation; d) deconvolution of emission spectra measured under 295 nm excitation.

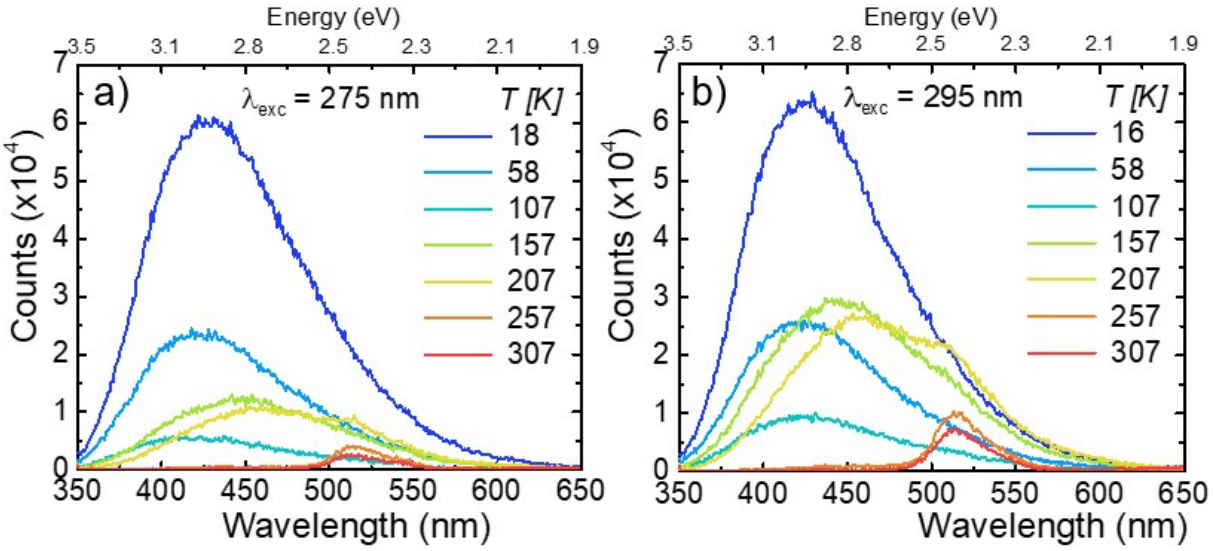

Figure S3. Persistent luminescence spectra of $Zn_{2.91}Ga_2Ge_2O_{10}$ at different temperatures measured after 10 min irradiation with a) 275 nm, b) 295 nm.

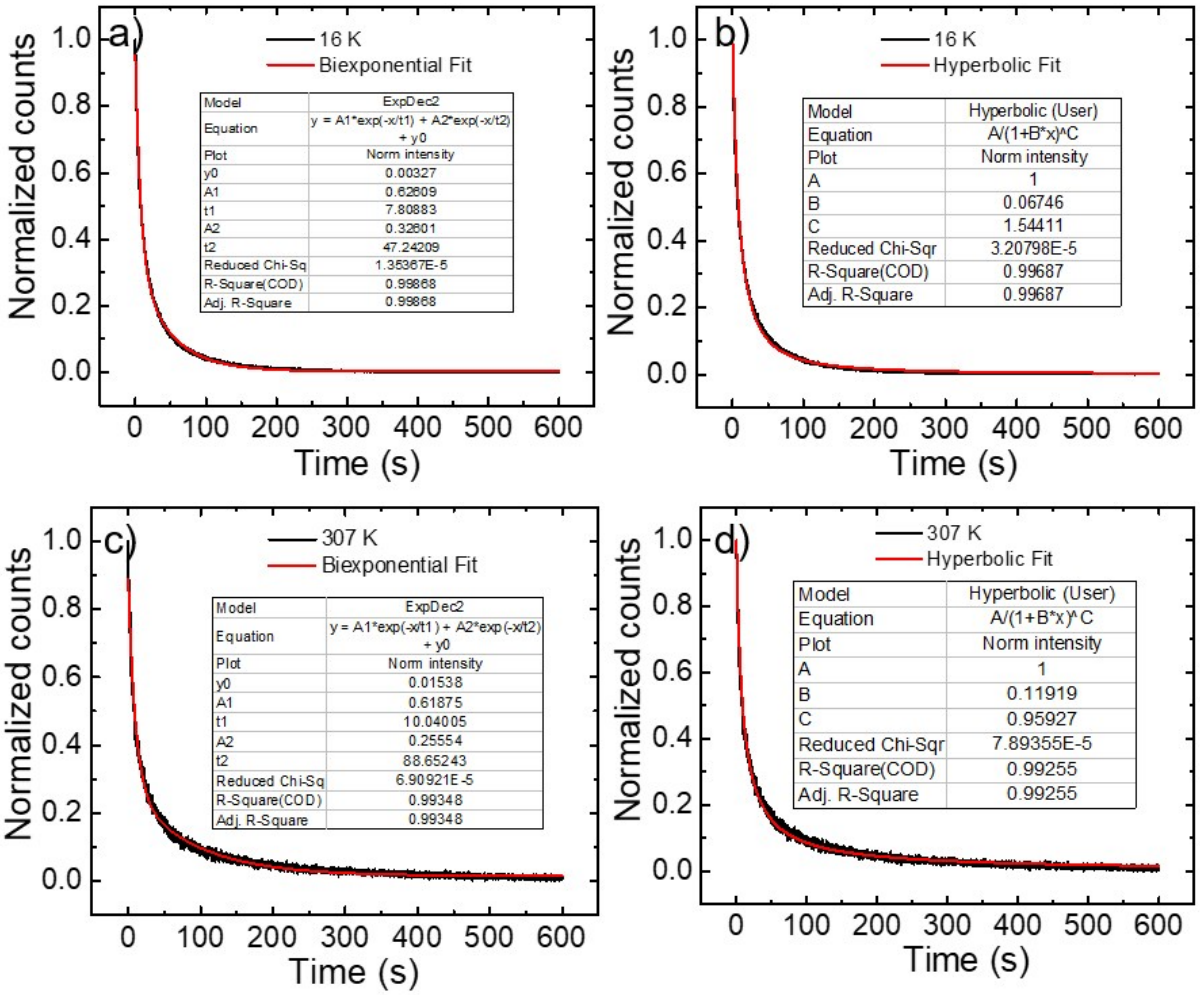

Figure S4. Selected persistent luminescence decays of $Zn_{2.91}Ga_2Ge_2O_{10}$ measured at different temperatures with biexponential and hyperbolic fits presented in Figure 4c,d,e. Prior to the fitting, all decay curves were normalized to the value of unity, i.e., the parameter *A* in Eq. 3 was set as unity in each case.

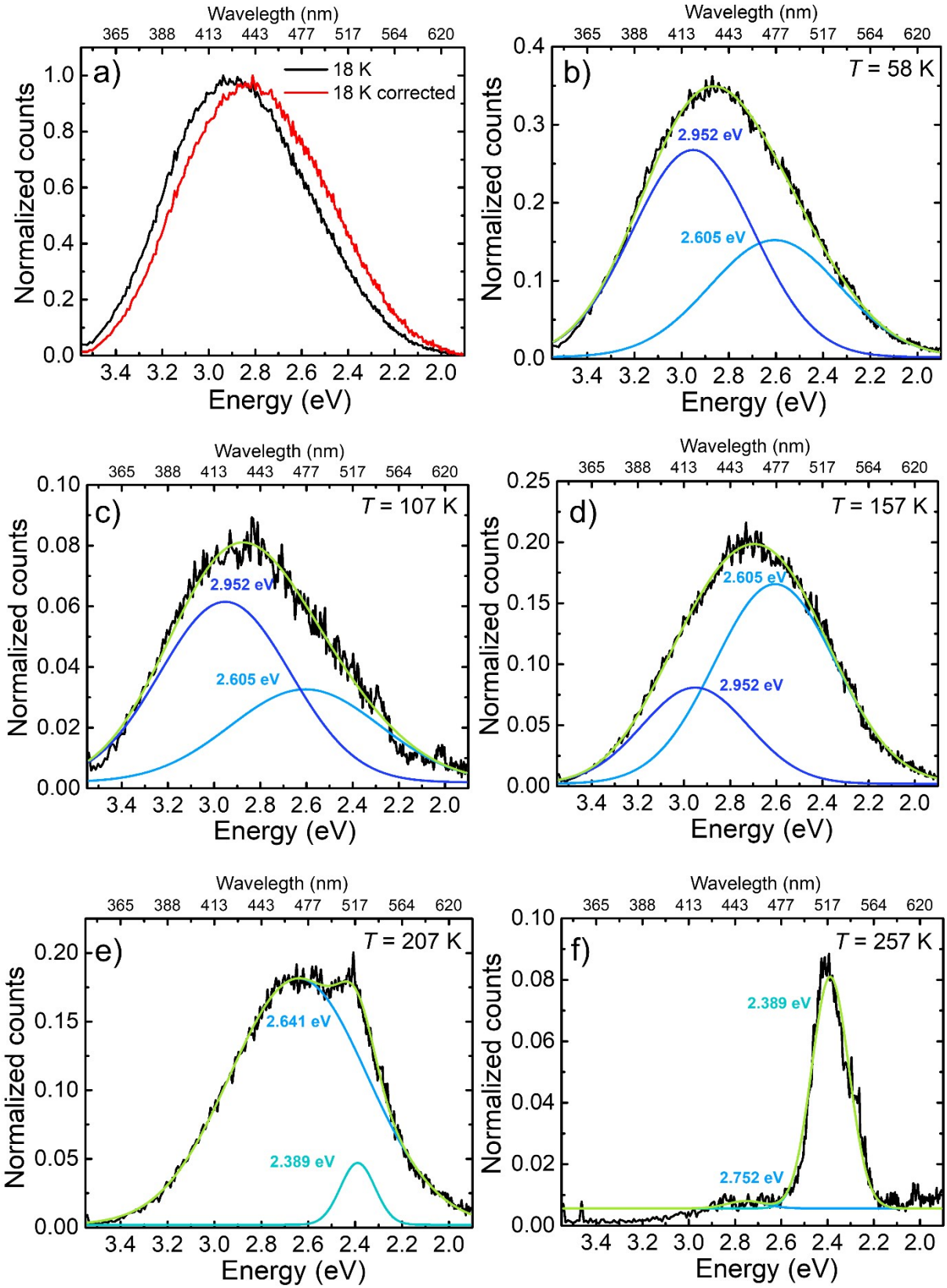

Figure S5. Deconvolution of persistent luminescence spectra of $Zn_{2.91}Ga_2Ge_2O_{10}$ at different temperatures: a) difference between original data and data corrected using Jacobian conversion; b) 58 K; c) 107 K; d) 157 K; e) 207 K; f) 257 K.

Before the deconvolution, the spectra were plotted on a wavelength scale. The Jacobian conversion was performed to an energy scale. The comparison between the spectra without and with Jacobian conversion is presented in Fig. S4a. The maximum of the corrected emission band has moved slightly to lower energy. The deconvoluted energies in Figures b-f correspond to the following wavelengths: 2.389 eV (519 nm); 2.605 eV (476 nm) and 2.641 eV (470 nm); 2.952 eV (420 nm).

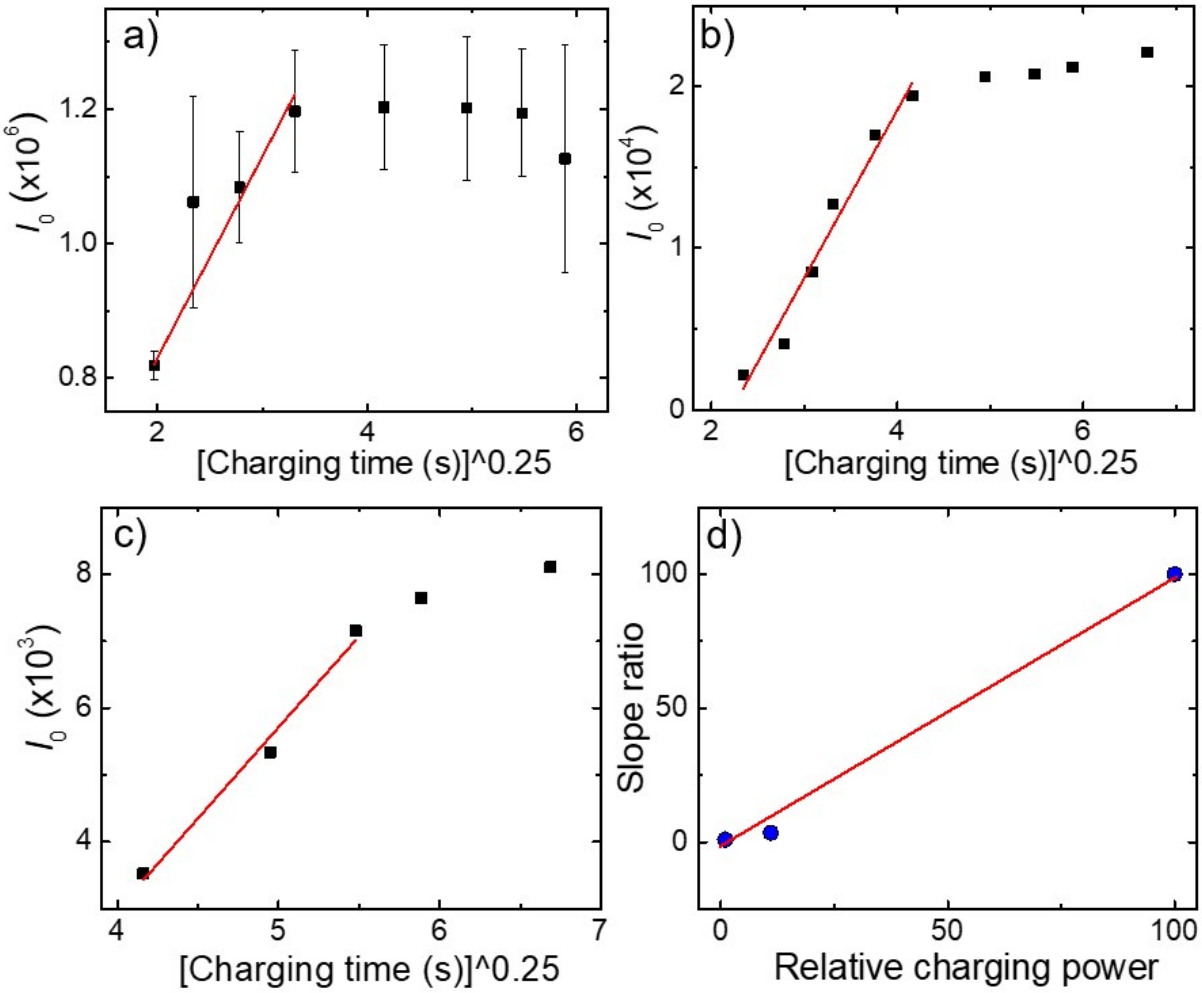

Figure S6. Fits of the initial charging regime of $Zn_{2.91}Ga_2Ge_2O_{10}$ at 10 K using 275 nm radiation according to Eq. S3 for (a) 100% power, (b) 11% power, and (c) 1% power. (d) Plot of the ratio of the slopes in Figures a-c against relative charging power. The red line is not fitted but is drawn to show a linear relation.

Comment upon Figures 6e)-g)

The fitted values of C are plotted against charging time in Figure 6e. A reasonable fit with $R_{adj}^2 = 0.9862$ is obtained for an inverse proportionality of C with charging time, t: $C = (1.764 \pm 0.007) + (9.35 \pm 0.42)/t$. However, if the Eq. S2 is strictly followed and the value 1.764 is instead constrained to 1, the fit is poor after about 50 s. This timescale was associated with saturation in Figure 6a.

Both of the parameters B and C were varied in the datafits to Figures 6f,g. In Figure 6f, the parameter C has a clear increasing trend with increasing charging power, with values changing from 1.34 to 1.79. According to Eq. S4, the relationship between B and charging power should be linear. This relation is not clearly observed in Figure 6f, above the first two points. Finally, Figure 6g presents the changes of fitting parameters with the delay time. The parameter B decreases with the increase of the delay time and can be fitted with an inverse relationship ($B = A_1 + A_2/t$, $R_{adj}^2 = 0.991$). On the other hand, the change of C parameter with increase of the delay time is not clearly characterized.

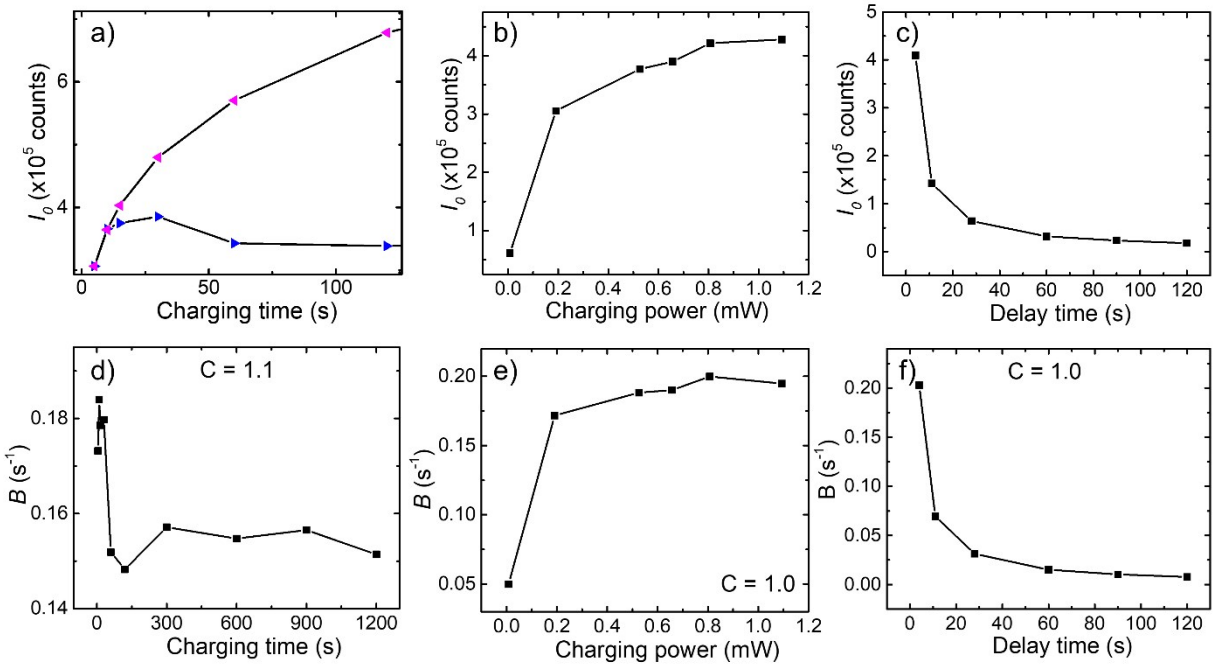

Figure S7. Parameters derived from persistent luminescence decays of $Zn_{2.91}Ga_2Ge_2O_{10}$ for different charging time, charging power and delay time at room temperature. The lines are a guide to the eye (λ_{irrad} = 275 nm; λ_{em} = 520 nm); a) comparison between results of initial counts as a function of charging time obtained from experiment (blue curve) and initial counts calculated using equation S3 (curve with pink triangles); b),c) initial counts as a function of charging power and delay time, respectively. The decays for charging time, power and delay time can be well-fitted with constant C parameter (C = 1.1 ± 0.0 in d, and C = 1.0 ± 0.0 for e,f) and varying B parameter.

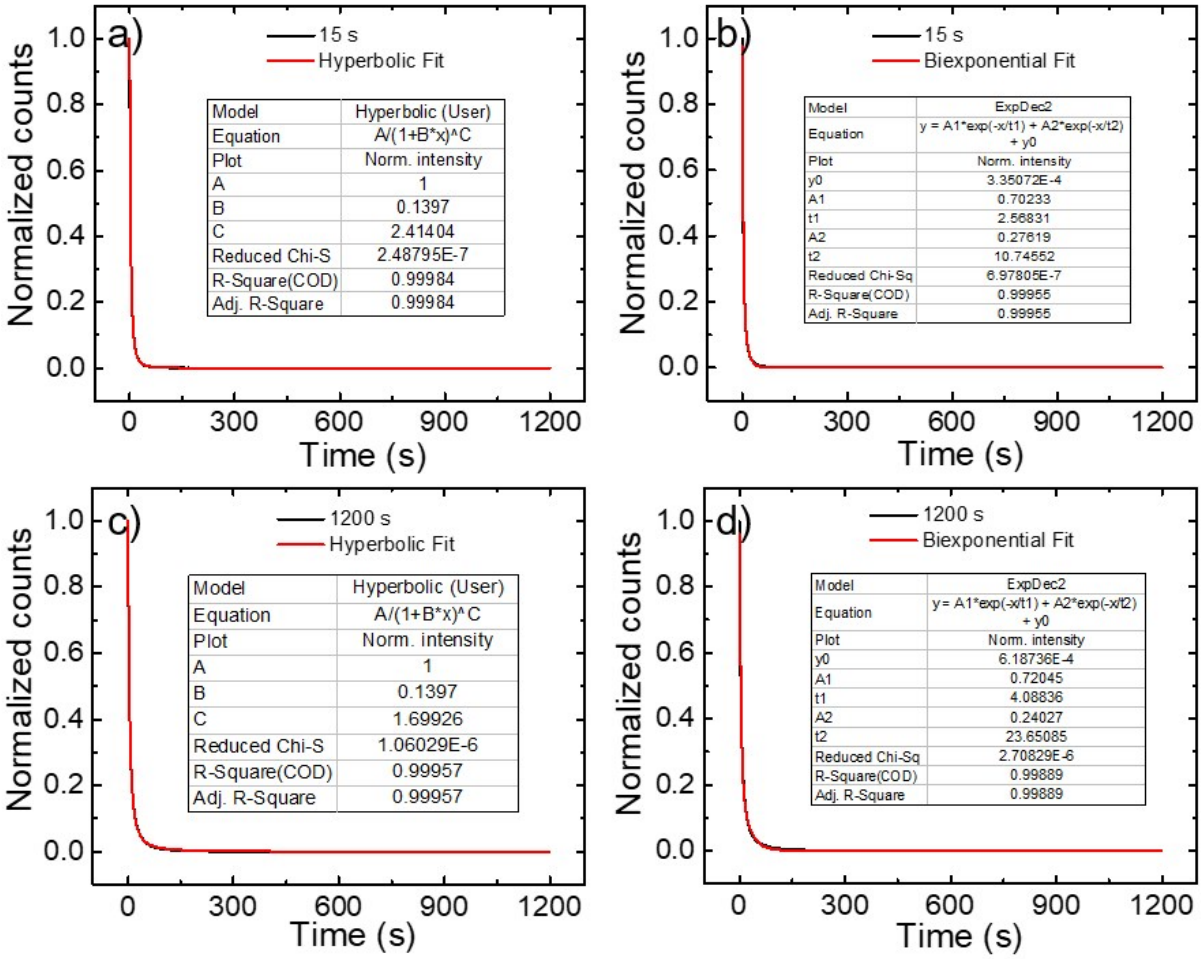

Figure S8. Selected persistent luminescence decay curves at 10 K (λ_{irrad} = 275 nm; λ_{em} = 425 nm) fitted by biexponential and hyperbolic functions. Prior to the fitting, all decay curves were normalized to the value of unity, i.e., the parameter *A* in Eq. 3 was set as unity in each case. The decays obtained for different charging times can be fitted by the hyperbolic function Eq. 3 with only one variable parameter *C*, while $B = 0.1397$ is kept constant.

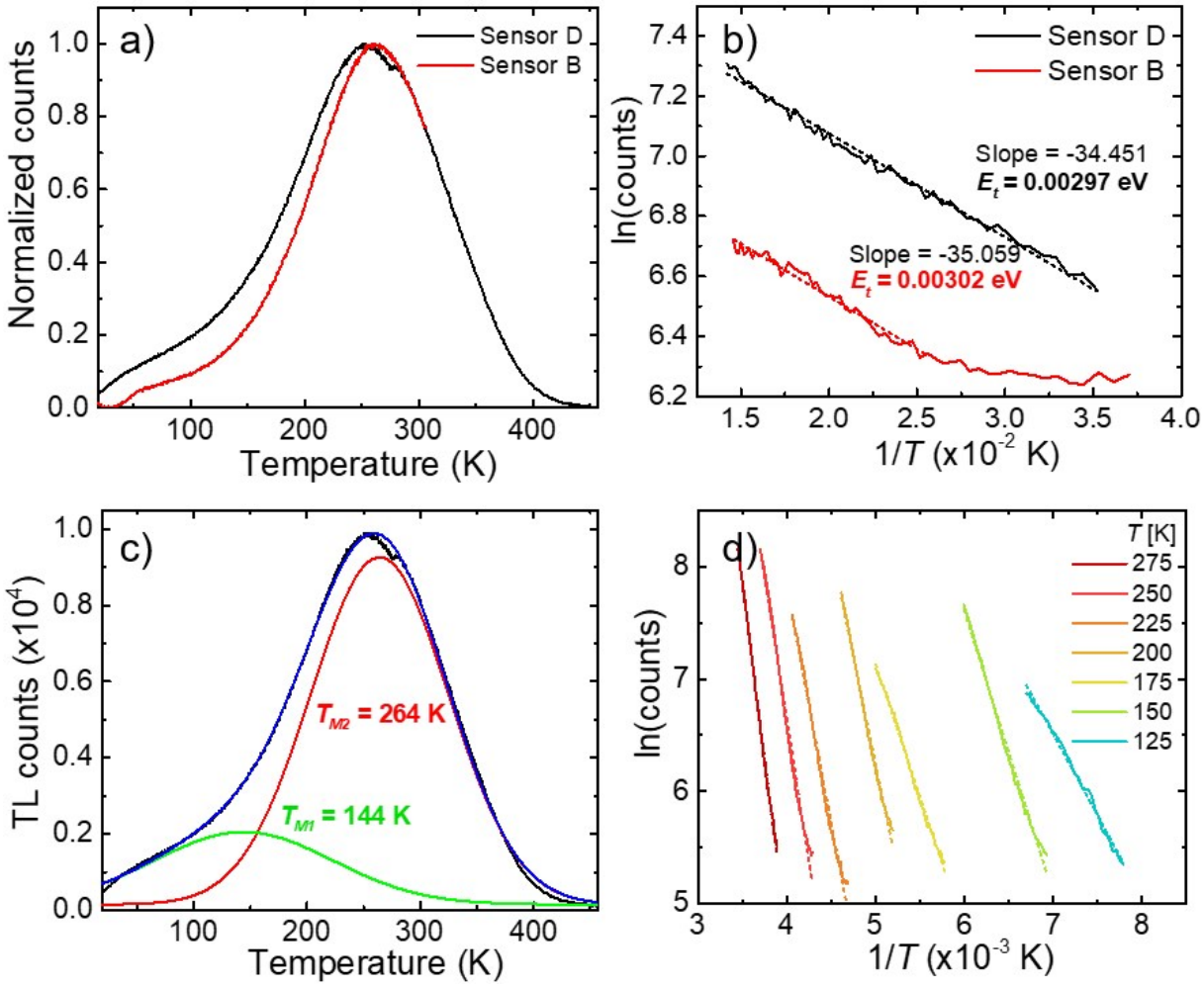

Figure S9. Thermally Stimulated Luminescence (TL) of $Zn_{2.91}Ga_2Ge_2O_{10}$: a) TL glow curve monitoring 517 nm emission (uncorrected for thermal quenching) recorded using alternative temperature sensors in the cryostat. b) Application of the initial rise method to the glow peak at 144 K (Figure 7b). c) Fitting of glow curve by two Gaussians and d) Initial rise method applied to Figure 8b for the low temperature peak (T_{M1} 144 K in Figure S8c).

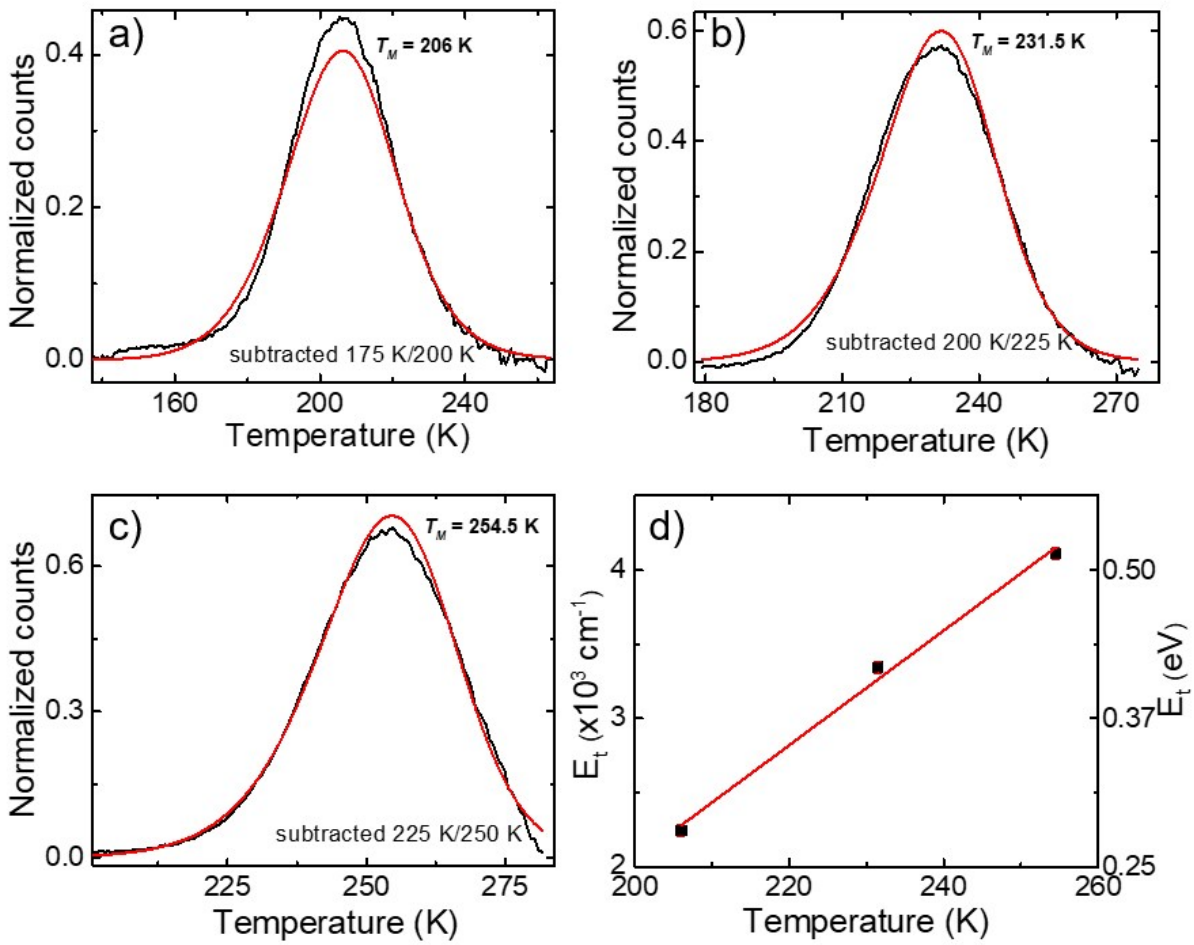

Figure S10. a)-c) Subtracted cleaned TL glow curves presented in Figure 8 and d) fitted with Eq. S5.

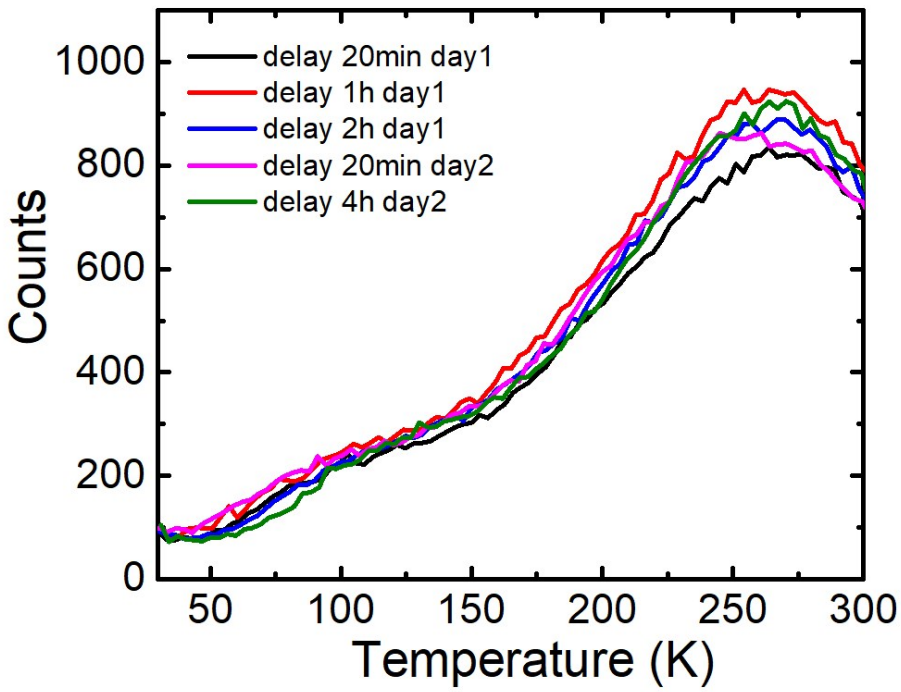

Figure S11. TL glow curves of $Zn_{2.91}Ga_2Ge_2O_{10}$ measured after various delay times between the end of irradiation and the beginning of TL recording.

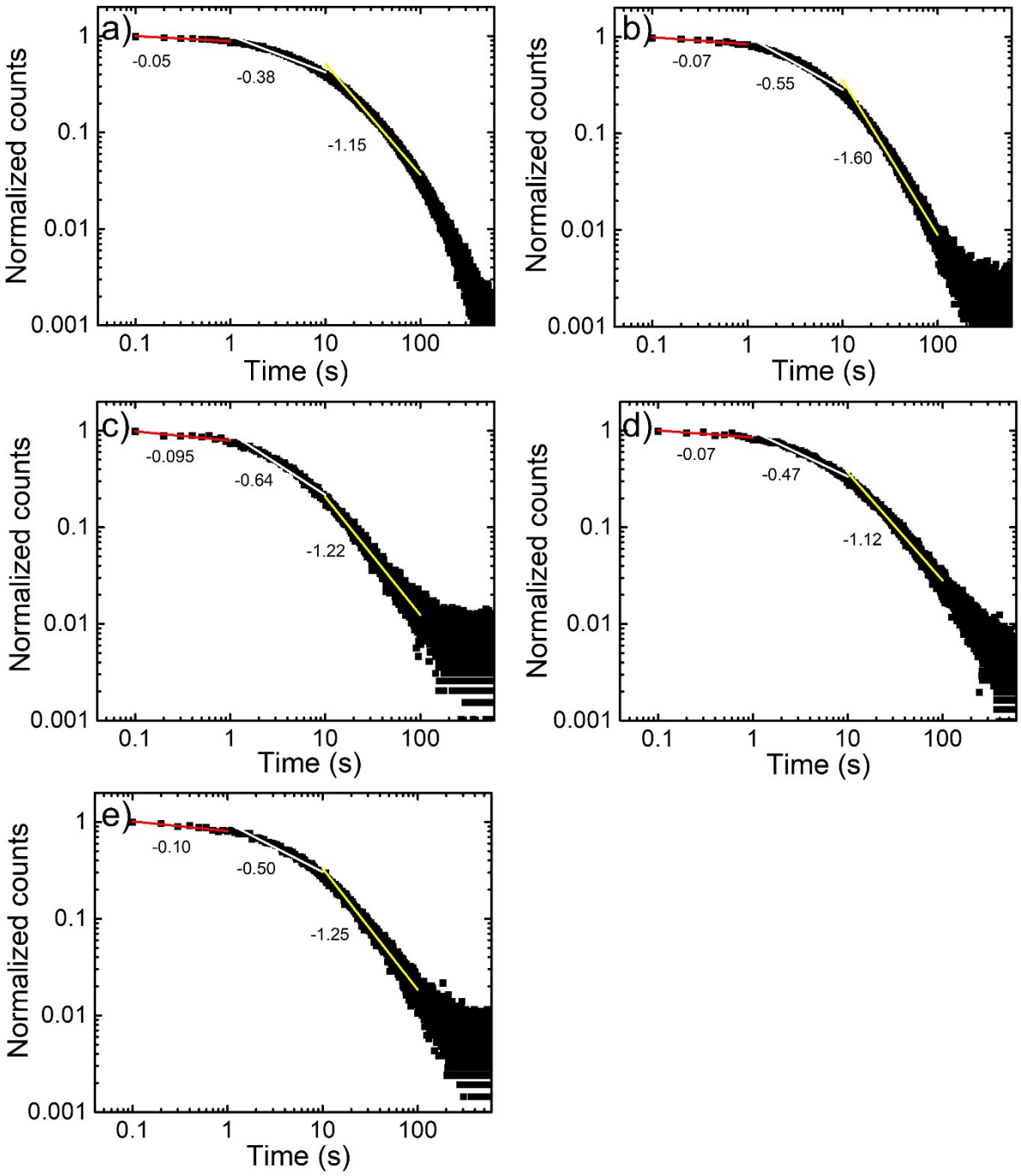

Figure S12. Power law decay fitting of decay curves (λ_{irrad} = 255 nm, λ_{em} = 400 nm) recorded at different temperatures for $Zn_{2.91}Ga_2Ge_2O_{10}$. The slopes are indicated from 0.1-1 s (red), 1-10 s (white) and 10-100 s (yellow). a) 16 K; b) 58 K; c) 107 K; d) 157 K; e) 207 K.

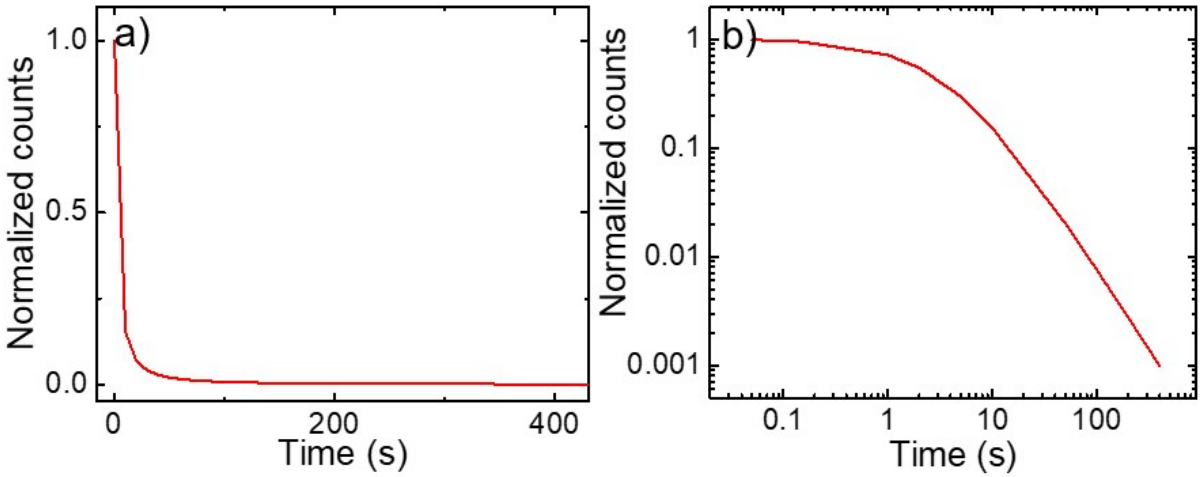

Figure S13. Relationship between hyperbolic and power laws: a) the plot of Eq. 3 with c = 1.5, b = 0.25, with the initial intensity A set to 1. b) The same data is presented as a power law, Eq. 4, using a log-log scale. The exponent a (slope of the curve) is only constant at long times and low counts.

Table S1. Fitted biexponential lifetime parameters from room temperature photoluminescence decays of $Zn_3Ga_2Ge_2O_{10}$ measured using ns excitation (λ_{exc} = 269 nm). The *Range* refers to the measurement time range for fitting. A_1 and A_2 are the contributions of the respective lifetimes.

λ_{em} (nm)	λ_{em} (eV)	*Range* (ns)	τ_1 (ns)	A_1	τ_2 (ns)	A_2	A_1/A_2	R_{adj}^2
450	2.76	3200	23.6±0.3	2260±17	411±5	819±6	2.8	0.9782
		6500	22.5±0.4	4281±38	374±5	1521±14	2.8	0.9858
470	2.64	3200	18.2±0.2	4484±32	405±4	1362±9	3.3	0.9795
		6500	17.3±0.3	3473±32	365±5	985±9	3.5	0.9823
515	2.41	3200	11.9±0.1	3720±28	394±6	603±6	6.2	0.9652
		6500	11.8±0.2	3086±28	345±7	472±6	6.5	0.9758

Table S2. Calculated power coefficients *a* for various time windows for log-log plots of persistent luminescence of $Zn_{2.91}Ga_2Ge_2O_{10}$.

λ_{irrad} (nm)	*T (K)*	*Slope at 0.1-1 s*		*Slope at 1.0-10 s*		*Slope at 10-100 s*	
		Power *a* in Eq. 4	R_{adj}^2	Power *a* in Eq. 4	R_{adj}^2	Power *a* in Eq. 4	R_{adj}^2
275	18	0.064±0.009	0.8418			1.241±0.005	0.9831
	58	0.077±0.007	0.9261			1.631±0.007	0.9831
	107	0.137±0.011	0.9418			1.359±0.010	0.9557
	157	0.096±0.016	0.7953			1.211±0.007	0.9735
	207	0.085±0.017	0.9547			1.293±0.009	0.9547
255	16	0.053±0.008	0.829	0.376±0.008	0.9581	1.150±0.005	0.9843
	58	0.073±0.010	0.8629	0.5472±0.012	0.9591	1.601±0.007	0.9840
	107	0.095±0.020	0.7058	0.6394±0.014	0.9594	1.222±0.009	0.9508
	157	0.074±0.018	0.6464	0.4669±0.010	0.9595	1.118±0.005	0.9805
	207	0.1006±0.012	0.8905	0.5045±0.011	0.9576	1.2532±0.007	0.9700
295	16	0.040±0.004	0.9217	0.3346±0.007	0.9617	1.0711±0.005	0.9814

References

1. Gouda, K. & Hama, Y. Tunneling recombination luminescence of glassy polyethylene adipate γ-irradiated at low temperature and effect of electron scavengers. *Radiat. Phys. Chem.* **26**, 285–294 (1985).

2. Hama, Y. & Gouda, K. Initial distribution and tunneling recombination of cation-electron pairs in irradiated rigid materials as studied by TL measurement. *Radiat. Phys. Chem.* **21**, 185–190 (1983).

3. Kitis, G. TL glow-curve deconvolutionfunctions for various kinetic orders and continuous trap distribution: acceptance criteria for E and s values. *J. Radioanal. Nucl. Chem.* **247**, 697–703 (2001).